

DID YOU KNOW

WE HAVE A PSC SCALE-UP SOLUTION FOR YOUR PROCESS DEVELOPMENT WORKFLOW?

Gibco™ StemScale™ PSC Suspension Medium uses a spheroid self-assembly method to promote maximum expansion of pluripotent stem cells (PSCs) in suspension via an easy-to use, scalable protocol without the need for microcarriers.



Find out more at thermofisher.com/stemscale

gibco

Adipose micro-grafts enhance tendinopathy healing in ovine model: An in vivo experimental perspective study

Angela Palumbo Piccionello¹  | Valentina Riccio¹ | Letizia Senesi² | Antonella Volta³ | Luca Pennasilico¹ | Riccardo Botto¹ | Giacomo Rossi¹ | Adolfo Maria Tambella¹  | Livio Galosi¹  | Carlotta Marini¹ | Cecilia Vullo¹ | Antonio Gigante⁴  | Barbara Zavan⁵  | Francesco De Francesco²  | Michele Riccio² 

¹School of Biosciences and Veterinary Medicine, University of Camerino, Matelica, Italy

²Department of Plastic and Reconstructive Surgery-Hand Surgery Unit, Azienda 'Ospedali Riuniti' Ancona, Ancona, Italy

³Department of Veterinary Medicine Science, University of Parma, Parma, Italy

⁴Clinical Orthopaedics, Department of Clinical and Molecular Science, Polytechnic University of Marche, Ancona, Italy

⁵Department of Morphology, Surgery and Experimental Medicine, University of Ferrara, Ferrara, Italy

Correspondence

Francesco De Francesco, MD, Department of General and Specialties Surgery, SOD of Reconstructive Surgery and Hand Surgery, AOU "Ospedali Riuniti" di Ancona, Via Conca 71, 60126 Ancona, Italy.

Email: francesco.defrancesco@ospedaliriuniti.marche.it

Abstract

In Europe, approximately 100 000 to 500 000 tendon repairs are performed every year. These procedures are associated with a considerable rate of postoperative complications (from 6% to 11%). Autologous micro-grafts (AAMG) and stromal vascular fraction (SVF) have been shown to improve tendon healing in 60% to 70% of treated rodents. The purpose of this study was to evaluate the effects of AAMG in a sheep model with tendinopathy. We used sheep models because, as a large animal, they are more comparable to humans. The hypothesis was that SVF injection would improve tendon healing compared with the control group, reducing inflammatory and matrix degrading, while increasing anti-inflammatory expression and collagen synthesis in the early stage of tendon injury. Sixteen Apennine sheep aged 2 to 5 years underwent 500 UI type I collagenase injection into both common calcaneal tendons (CCT) to induce tendinopathy. After 15 days (T0), one CCT in every ovine underwent randomly to 2.5 mL of AAMG obtained by mechanical disruption and the contralateral CCTs received no treatment. Clinical, ecographic, and sonographic evaluations were performed after 4 weeks (T1) and 8 weeks (T2). Histological, immunohistochemical, real-time polymerase chain reaction (RT-PCR), and biomechanical evaluations were performed at T2. At T2, the treated group showed a final tendon diameter (9.1 ± 1.4 mm) and a hardness expression (62%) that were similar to the original healthy tendon (8.1 ± 1.1 mm; 100%), with a significant recovery compared with the control group (9.5 ± 1.7 mm; 39%). Moreover, histological analysis of the treated group revealed an improvement in the fiber orientation score, fiber edema score, infiltrative-inflammatory process, and necrosis score (4.3 ± 3.3) compared with control group (8.8 ± 2.9). Immunohistochemically, the treated group showed high expression of collagen 1, Factor

Angela Palumbo Piccionello and Valentina Riccio contributed equally to this study.

Francesco De Francesco and Michele Riccio are equally senior authors.

This is an open access article under the terms of the Creative Commons Attribution-NonCommercial-NoDerivs License, which permits use and distribution in any medium, provided the original work is properly cited, the use is non-commercial and no modifications or adaptations are made.

© 2021 The Authors. STEM CELLS TRANSLATIONAL MEDICINE published by Wiley Periodicals LLC on behalf of AlphaMed Press.

VIII and significantly low expression of collagen 3. These data were confirmed by RT-PCR analysis. The study findings suggested that AAMGs obtained through mechanical disruption present a safe, efficient, and reliable technique, enhancing tendon healing.

KEYWORDS

adipose derived stem cells, stromal vascular fraction, tendinopathy, tendon injuries, tendon regeneration

Significance statement

The group treated with stromal vascular fraction showed a final tendon diameter and a percentage hardness expression that were similar to the original healthy tendon.

1 | INTRODUCTION

According to the World Health Organization (WHO), musculoskeletal disorders (MSDs) are a major cause of disability worldwide.^{1,2} MSDs include tendon disorders due to biomechanical overload (acute) or degenerative and enduring conditions (chronic)^{3,4} with an overall incidence rate of approximately 30%.^{5,6}

These lesions are common in adults and adolescents engaged in vigorous physical activity, in a population participating in moderate physical activity, and in an elderly inactive population.⁷ Acute tendon ruptures are characterized by a sudden onset of pain and loss of function, whereas chronic tendon injuries present with a progressively increasing sensation of pain and loss of function. Chronic tendon injuries are characterized by irreversible structural change in tendon structure with management of these lesions thus posing an important clinical challenge.

Approximately one third of people affected are nonathletes who are often compelled to prolong absence from work, which has a marked financial impact on society.⁸ Moreover, 84 000 Europeans are affected by these injuries annually, 30% of whom undergo surgical interventions.⁹ A systematic review revealed that tendon degeneration is a consequence of insufficient adaptation of the matrix and remodeling considering the disproportionate matrix decomposition and synthesis caused by stress and mechanical loads, characterized by excessive tenocyte proliferation, an increase in non-collagenous matrix, abnormal crimping and loosening as well as an increased waviness of the collagen fibers shift to a higher collagen-3 (COL3) abundance, considering collagen-1 (COL1) in the extracellular matrix (ECM) (about two to three times more).¹⁰ In a recent systematic review Jomaa et al. affirmed that several inflammatory mediators are involved and intensified in tendinopathies, as well as engagement of growth factors.¹¹ These mechanisms cause permanent disorder and fundamental alterations in structure and composition, cell death, tissue collapse and dysfunction with potential to exacerbate lesions and ruptures.¹⁰ Moreover, the ability of tendons to heal spontaneously and regenerate original tissue is effectively inefficient due to prolonged tendon repair and subsequent scar tissue development.¹² Indeed, an elastosonographic study performed in humans

after Achilles' tendon rupture, compared with contralateral one, showed that healed Achilles' tendon after rupture has inferior elastic properties even after a long-term healing phase of 2 years (shear wave velocity 1.2 ± 1.5 m/s) compared with control groups 2.5 ± 1.5 m/s). Differences in elastic properties after rupture mainly originate from the mid-substance of the Achilles tendon, in which most of the ruptures occur.¹³ At present, several reviews and systematic reviews of studies performed in humans report that nonoperative treatments such as drug medications,¹⁴ shock wave therapy,^{15,16} physio-kinesiotherapy,¹⁷ and operative treatments such as injectable therapies^{18,19} or surgical treatments²⁰⁻²² are available. Unfortunately, current and traditional treatments often provide inadequate pain management and, therefore, are unable to restore original structure, tendon functionality, and biomechanical characteristics.²³

The use of nonsteroidal drugs and corticosteroids is considered controversial but remains a mainstay in the clinical treatment of tendinopathy. As aforementioned, inflammation is not the cause but the consequence of tendinopathy and these drugs provide a limited effect on tendon degeneration. A recent review showed that corticosteroids are known to inhibit the synthesis of collagen, which in addition to the masking of pain and consequent recovery of the load will eventually result in tendon atrophy or rupture of the tendons^{23,24} (side effects reported in 82% of corticosteroid trials).²⁵

For decades, surgeons have argued, despite the lack of general consensus in the literature, that rest, consolidated physiotherapy exercises (as first-line management given the satisfactory results in 25-45% of cases), and surgery (as a final option) are gold standard managements for tendinopathy.²⁵ Surgical interventions may be an option in restoring or substituting the injured tendon using direct suture or autograft,²⁶ allografts, xenografts, or prosthetics.^{27,28}

Nevertheless, inflammation and suture retention weakness prevent an optimal clinical outcome and the increase in treatment cost is to be acknowledged.²⁹ Indeed, the increased incidence rate and ineffective treatments of MSDs have resulted in a rise of up to \$874 billion from 2000 to 2015.^{30,31} These pathologies represent an important socioeconomic burden on worldwide healthcare; hence, an effective and affordable therapeutic plan is surely imperative.

Recently, regenerative medicine, a novel multidisciplinary area of research employing biomaterials, growth factors, and stem cells, has earned ample attention on behalf of the scientific community, mostly related to the regenerative and rejuvenating characteristics concerning diseased or senescent cells, tissues, or organs.³²

Regenerative tendon procedures have been investigated in several review as cellular therapy³³; platelet concentrates such as platelet-rich plasma (PRP) injections,^{34,35} gene therapy,³⁶ and biomaterial-based techniques.³⁷ Adipose-derived stem cells (ASCs) are a type of mesenchymal stem cell commonly adopted in tissue engineering or cell therapy. In comparison with MSCs derived from the bone marrow, ASCs are readily isolated and accessible from the processing of adipose tissue. ASCs stimulate tissue regeneration by secreting cytokines and growth factors to promote normal tissue function and diminish tissue detriment.^{38,39} ASCs have been studied in recent systematic reviews in relation to treatment of osteoarthritis and tendinopathy conditions in humans, with significative improvements in the treated group.^{40,41}

In particular, Jo et al.⁴² showed a significant improvement in functional score (SPADI score increased from 77% to 81% in treated groups), pain (ameliorated in 71% of the treated group), radiological and arthroscopical findings (MRI examination revealed a decrease of 90% in the volume of bursal site in treated groups and, moreover, the volume of the articular- and bursal-side defects decreased from 83% to 90%) of shoulder in patients with rotator cuff disease after intratendinous injection of ASCs. Moreover, ASCs prompted the arrangement of collagen fibers in tendon lesion models, with a significative lower rate of collagen fiber type III in ASC group^{43,44} (ratio of type III collagen to type I collagen decreased over time in the ASC group, from 0.169 to 0.116).⁴⁴ ASCs have also differentiated into tenocytes with modulation of the inflammatory environment, promoting a regenerative/anti-inflammatory M2 macrophage phenotype, and influenced tendon ECM remodeling in rodent⁴⁵ and angiogenesis and cell survival in canine animal models (median increase in serum VEGF levels was observed 18.37 pg/mL, vs control group 10.37 pg/mL).⁴⁶

The Good Manufacturing Practice regulations of the European Parliament (EC regulation no. 1394/2007) state that only minimal cell manipulation is acceptable in a clinical context, thus precluding the use of enzymatic methods, especially in human trials.^{47,48} In line with these constrictions, companies have devised automatic closed devices appertaining to mechanical procedures⁴⁹⁻⁵² to isolate the stromal vascular fraction (SVF), which comprise ASCs, mesenchymal and endothelial progenitor cells, leukocytes, and pericytes. Adipose tissue can be mechanically destroyed obtaining autologous micro-grafts (AAMG). The process consists of a sterile procedure, without use of enzymes, where the adipose tissue is gently disaggregated by use of elicoidale blades in a sterile capsule.⁴⁷ This procedure is able to maintain the microenvironment of perivascular niche, while pro-inflammatory factors are removed. The residual stromal vascular niche (or SVF) contain pericytes, that once detached from the capillary wall, are able to gradually convert into activated ASCs.^{53,54} AAMG obtained has been

demonstrated to have a great anti-inflammatory and healing effects applied in MSDs.^{52,55} Moreover, over PRP and bone-marrow aspirate, the procedure is easier, faster, safe, and reliable, with less morbidity to donor site.⁵⁶

Polly et al. demonstrated an association of SVF and ASC to tendon healing, in vitro on the flexor digitorum superficialis tendon in horses. Both SVF and ASC expressed essential growth factors in tendon healing.⁵⁷ Behfar et al.,⁵⁸ in their in vivo and in vitro study in rabbits, showed that SVF from subcutaneous adipose tissue promoted histological, immunohistochemical, and biomechanical flexor tendon healing with improved ultimate tensile strength (18.92 ± 1.49 N/mm² vs 4.7 ± 2.48 N/mm²), in addition providing a source of cells with stimulatory potential in tendon regeneration.⁵⁹⁻⁶¹ Additionally, SVF administration has yielded positive results in rotator cuff tears in rabbits, accelerating regeneration of "bone-cartilage" in the interface during the healing of rotator cuff insertion evaluated through immunohistochemical (type I collagen/type III collagen area ratio of the experimental group 1.69 ± 0.43 was significantly increased, compared with that of the control group 1.31 ± 0.34 , and BMP-2 value (64.5 ± 3.8) was markedly enhanced, compared with that of the control group (46.8 ± 3.4) and biomechanical analysis (maximum load 166.89 ± 11.62 N in treated group vs 99.4 ± 5.70 N in control group).⁶¹ SVF administration in non-insertional Achilles tendinopathies in humans promoting significative tendon vascularization and thickness evaluated through ultrasound and magnetic resonance (US size 9.9 ± 3.2 mm 10.7 ± 3.1 mm MR size 10.2 ± 3.3 mm 10.7 ± 3.3 mm).⁶² Usueli et al.⁶³ found that both PRP and SVF were safe, effective treatments for recalcitrant non-insertional Achilles tendinopathies in humans, with SVF offering more rapid functional outcomes within 15 days after treatment (VAS 4.8 vs 2.8; AOFAS 80 vs 65).

The articles mentioned above have the following levels of evidence References 10 and 11: I/II; References 12, 14-21, and 24: II/III; References 13, 25-28, 33-37, 42-45, 54, 56, 57, and 62-63: III/IV.

The hypothesis of our study was that AAMG administration would promote healing and functional and original tendon structure recovery in terms of fibers orientation, ultrasonographic evaluation, and genic expression in the treated tendon compared with the control tendon, thanks to their intrinsic anti-inflammatory activity.

Therefore, we believe this treatment represents a safe, reliable, and more effective treatment in tendinopathy, with a lower rate of postintervention complications, strengthening the actual indication of their employment also in human tendinopathy.

2 | MATERIALS AND METHODS

2.1 | Animals

Sixteen female sheep (Appenninica) aged between 2 and 5 years, weighing between 50 and 60 kg were selected for the study.

At the beginning of the study, four sheep were randomly assigned to final biomechanical analysis. The remaining 12 animals underwent ultrasonographic, histological, and immunohistochemical evaluation. The sheep allocated to biomechanical analysis were monitored via ecographic and elastosonographic follow-up.

Seven days before the experiment, the animals were stabulated in special stands in accordance with current legislation (Table 7.2 Annex III, DL 26/2014). Animals were submitted to clinical (general, orthopedic, and neurological) assessments, as well as ultrasonographic and elastosonographic analysis before the experiment, to ensure absence of tendon injuries. A complete blood count was also performed to confirm the health status of the animals.

The inclusion criteria were as follows: anesthesiologic risk class (ASA) I; absence of orthopedic and neurological disease, including previous tendon injury; normal blood sample analysis; and no pregnancy or lactation status.

The protocol was approved by the Italian Ministry of Health (authorization number 620/2018-PR).

2.2 | Study design

The study envisaged the formation of an equal bilateral iatrogenic lesion in both common calcaneal tendons (CCT) through collagenase type I injection (Ti), and treatment of one limb with autologous SVF (T0). The healing process was monitored for 8 weeks, comparing the treated limb with the untreated limbs (T1-2). The 24 tendons (CCT) were randomly allocated to the treatment group (12) or to the control group (12), thereby assigning one common calcaneus tendon of each sheep to the treatment group and the contralateral tendon to the control group. Adipose tissue from the subscapular site was collected 15 days after lesion induction (T0), and contextually SVF was administered to the treated group. Clinical examination, sonographic and elastosonographic assessments were performed prior to lesion induction (Ti), on treatment day (T0), after 4 weeks (T1), and after 8 weeks (T2). The animals were sacrificed following 8 weeks of treatment and a biopsy of the CCT in the treated group and control group was performed for histopathological and immunohistochemical evaluations. All assessments were conducted by masked investigators who were unaware of study settings.

2.3 | Induction of tendon lesion

At Ti, sheep were sedated by intramuscular administration of 0.3 mg/kg of Midazolam (Midazolam) and 15 µg/kg Buprenorfine (Buprenodale) and then placed in lateral recumbency. All subjects underwent bilateral B-Mode ultrasound and elastosonography (Mylab Class C, Esaote, Genova, Italia) of the common calcaneal tendons and on termination of the ultrasound, bilateral CCT injury was induced by inoculation of 500 U of type IA collagenase (Sigma, St. Louis, Missouri) under ultrasound control (Mylab Class C, Esaote, Genova, Italia) in the center of the affected tendon, 6 cm proximal to the calcaneal tuberosity, using a 22 G needle (Figure 1A-C).

2.4 | Collection and application of adipo-micro-graft

Two weeks following lesion induction (T0), the animals underwent surgical procedures for adipose tissue harvesting. After sedating the subjects with Midazolam and Buprenorfine (0.3 mg/kg and 15 µg/kg, respectively), induction was conducted maintaining intravenous anesthesia with propofol, a local trichotomy was then performed at the intrascapular area appropriately sterilized using alternating scrubs of povidone iodine and alcohol, the surgical area was covered with a sterile adhesive barrier. Four grams of subcutaneous fat were harvested and immediately processed with Rigenera (Human Brain Wave, Torino, Italia) (Figure 1D). The vascular-stromal fraction (autologous adipose micro-grafts) thus obtained (2.5 mL) was inoculated after attentive disinfection, using a sterile syringe with a 22 G needle inserted, by ultrasound guide, at the center of the tendon lesion of each pelvic limb assigned to the treated group (Figure 1E). Tendons pertaining to the control group were not treated. At the end of the procedure all sheep received 15 000 IU/kg of procaine penicillin G (Depocillina; Msd Animal health Srl, Segrate [MI], Italia) and 1 mg/kg di flunixin meglumine (Finadyne, Intervet Italia Srl, Segrate [MI], Italia) injected muscularly immediately following the surgery and for 3 consecutive days postsurgery. The therapeutic procedure was repeated, once a day, for the following 4 days.

2.5 | Rigenera system

The Rigenera system consists of a motorized apparatus that allows a sterile and disposable capsule (Rigeneracons) to mechanically break up the tissue placed inside to obtain micro-grafts equally measuring 50 to 70 µm.³⁴⁻³⁷ Each Rigeneracons is internally made up of a helical blade managed by an electric motor that enables rotation at 80 rpm, thus allowing a precise, uniform and constant cut. In addition, a metal filter with 100 holes is located at the end of each propeller containing approximately 50 µ, each of which has six micro-scalpels. The segregated and filtered tissue is then collected from the bottom of the capsule, aspirated using an appropriate syringe and accordingly used (Figure 1D,E).

2.6 | Clinical assessment

The transversal diameter of the tendons with animals in orthostatic position was measured 6 cm from proximal calcaneal tuberosity with a caliber (Ti, T0, T1, T2) and expressed in mm (Figure 2).

2.7 | Ultrasonographic and elastosonographic evaluation

Ultrasonographic and elastosonographic evaluations were performed in all 24 tendons, at 6 cm from the calcaneus, prior to lesion induction

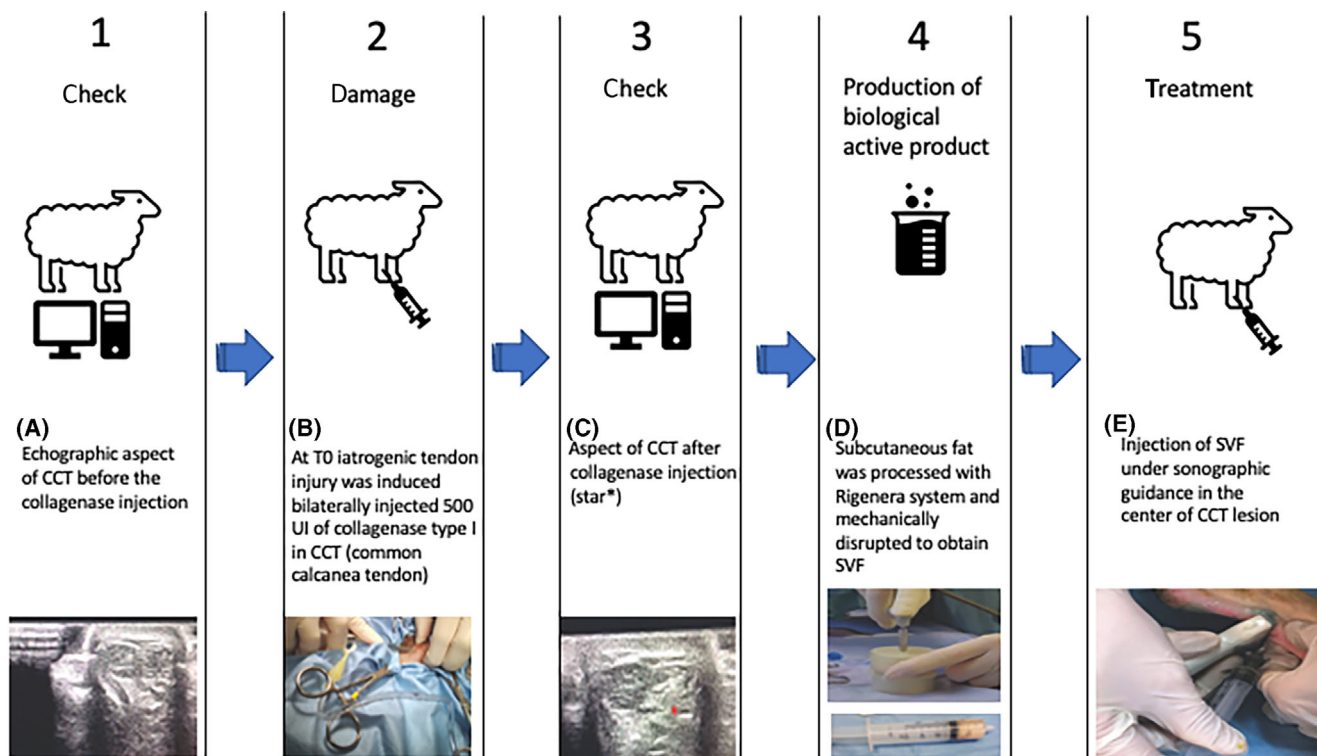


FIGURE 1 A, normal echographic image of CCT before the collagenase injection. At T_i iatrogenic tendon injury was induced bilaterally by 500 UI injection of collagenase type I in CCT through sonographic guidance (B) appearance of CCT after collagenase injection (star*) (C). At T₀, the autologous subcutaneous fat harvest from the interscapular area. Subcutaneous fat, processed with the Rigenera system and mechanically disrupted to obtain SVF (D). Injection of SVF under sonographic guidance in the center of the CCT lesion (E)

(T_i), on treatment day for the treated group (before administration) (T₀), after 4 weeks (T₁), and at the end of the experiment (T₂).

The real-time B-mode analysis was conducted using a 3-to-11 MHz multifrequency linear transducer set at 11 MHz (My Lab Class C, Esaote, Genoa, Italy).

Longitudinal and transversal images were collected via B-mode ultrasound to examine the ultrasonographic pattern of the tendon and to measure the tendon diameter.

Moreover, according to Archambault score⁶⁴ Supplementary Table 1, tendon lesions were classified as follows:

- Grade 1: normal tendon appearance (parallel echogenic lines in a fibrillar pattern, uniform in size and in echo texture);
- Grade 2: enlarged tendon (irregular margin, homogeneous echo texture);
- Grade 3: hypoechoic areas, with or without tendon enlargement.

In the transverse section the thickness of the tendon was also calculated, at 6 cm from the calcaneus, and expressed in millimeters.

Elastosonography was performed using the same ultrasound machine equipped with elastosonographic properties (ElaXto software, Esaote S.p.A., Genoa, Italy), performed with the same linear transducer. The subjects were examined in lateral recumbency with tarsus flexion at 90° and the knee neutrally positioned. Tendon hardness and healing in the treated group and control were assessed

according to a color grading map⁶⁵: blue (hard tissue); green (intermediate tissue); red (soft tissue). The software allowed for quantitative processing in regions of interest (ROI), to conduct subsequent statistical surveys. For each sample, two values were measured, drawing the ROI over the entire area of the tendon including Elax-t% SFT which indicates the percentage of softness in a ROI; Elax-t% HRD indicates the percentage of hardness in a ROI. The survey was blinded and entirely conducted by the same operator, an experienced sonographer.

2.8 | Tendon biopsy

Eight weeks after the start of treatment (T₂) a surgical exeresis of the common calcaneal tendons was performed. Following induction of general anesthesia and euthanasia of all sheep by overdose of barbiturate, all tendons were sterilely removed via incision at the insertional levels with the respective bone bases (calcaneus), sutured at one end with a plate bearing the identification number of the subject and duly marked according to right or left common calcaneal tendon, then stored for 72 hours in 10% buffered formalin for histological and immunohistochemical analysis (Figure 2) Subsequently, the tendons were divided into longitudinal sections of approximately 3 cm including the maximum lesion area, obtaining a total of two blocks from each sampled tendon. The tendons were longitudinally sectioned, in

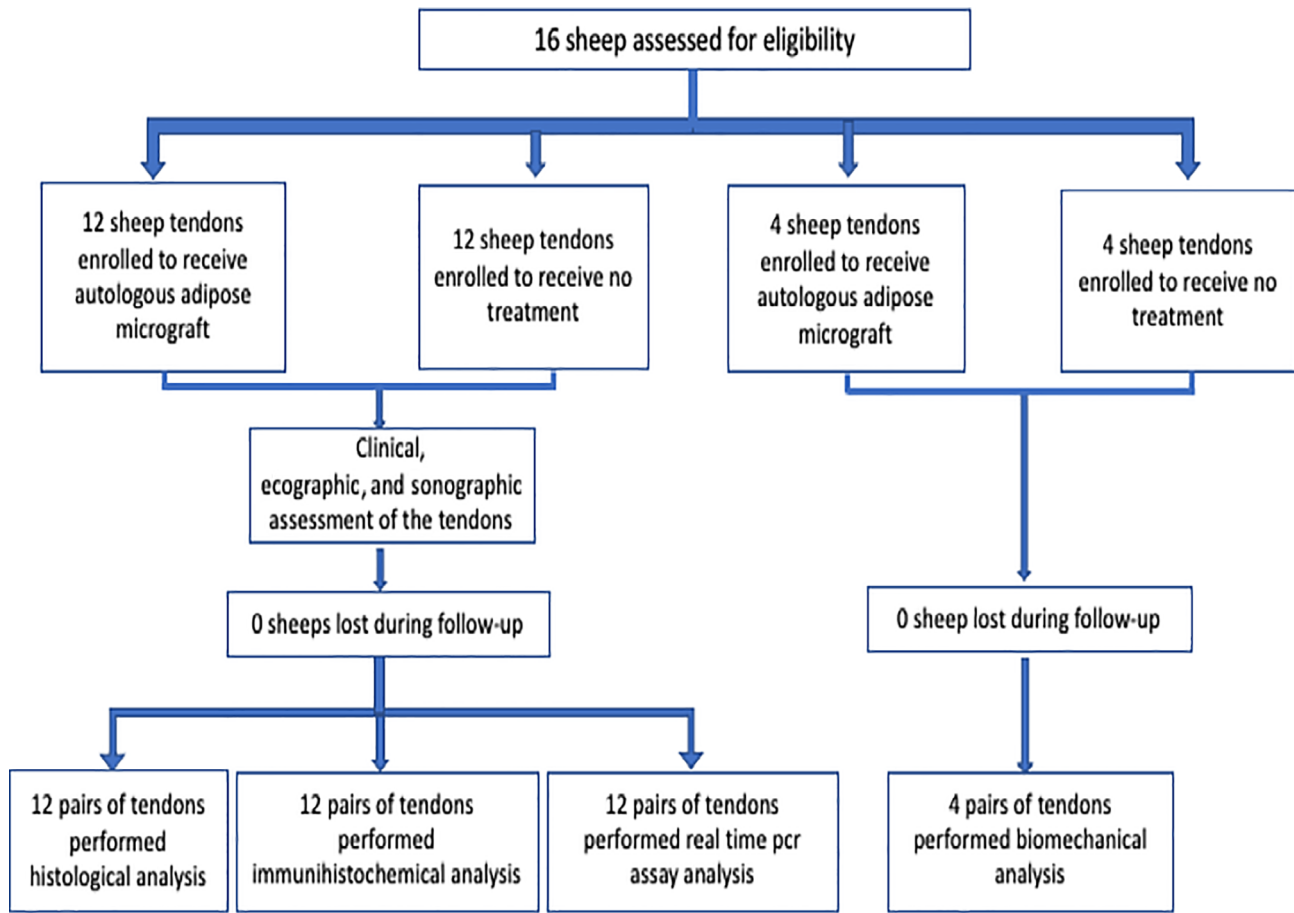


FIGURE 2 The graphic representation of the study design and of the animals involved

accordance with the arrangement of the collagen fibers and positioned in histological processing cages, then immersed in paraffin and cut with Leica microtome into thin 4 μm histological sections. The sections were then set onto electrostatic slides (Histoline, Milan, Italy) for maximum adhesion, allowed to dry and subsequently stained with Hematoxylin-Eosin. Histological and immunohistochemical assessment was performed blindly by a single operating pathologist. Histological examination of the tendon sections comprised evaluation of alignment areas of the collagen fibers in a longitudinal model, adopting a fiber orientation score (FOS). High FOS values are indicative of a greater degree of non-longitudinal or perturbed patterns and lower scores represent normal longitudinal patterns of the fibers according to the model: 3 (>75%), 2 (50-75%), 1 (25-49%), 0 (<25%), in which the percentages define the relationship between the damaged zone and the whole cross-sectional area of the common calcaneal tendon, as evaluated with a $10\times$ magnification. Considering the following parameters—predominant percentage of aligned; nonaligned; vortex or “fingerprint” organized fibers, we analyzed five randomly selected fields and assessed the score as the average percentage of the relevant fields.

Other strictly morphological evaluation criteria were also considered: the presence of edema/the myxoid aspect of the tendon area examined (*fibers edema score* = FES) (score 0-3), the presence of

necrosis (*necrosis score* = NS) (score 0-3) and the presence of an infiltrative-inflammatory process (FIIS), assessed according to the following score: from 0 to 3 inflammatory cells per field at 40x (score 0); from 3 to 5 cells per field (score 1); from 5 to 15 cells per field (score 2); over 15 cells per field (score 3). The final histological score was then expressed as the sum of the three scores (FOS + FES + FIIS + NS). The same evaluation parameters were adopted according to previous studies on tendon repair.^{46,66,67}

Regarding the consecutive tissue sections, diversely to sections on H&E evaluation, histochemical analyses were performed using Herovici's polychrome stain for pre-collagen and collagen differentiation.⁶⁶ Such procedure enables normal tendons to reveal a homogeneous composition of mature and intensely red staining fibrous collagen, and an optimal parallel alignment of the collagen fibers without infiltration of inflammatory cells between the fibers.

2.9 | Immunohistochemical evaluation

We deparaffinized the 4- μm -thick cuts with successive xylene baths and then rinsed them three times in pure alcohol and washed them in solutions with decreasing alcohol concentration (95% and 85%) before proceeding to incubation of the primary antibodies for COL1, COL3,

TGF- β 1, and Factor VIII. We blocked the endogenous peroxidase activity by using hydrogen peroxide (3%) in methanol for 20 minutes then washed them 10 times with distilled water. Following the peroxidase blocking, we proceeded to block nonspecific binding with 3% milk powder for 1 hour in a 27°C incubator, then rinsed the slides with TRIS solution. After dewaxing, we set the sections in EDTA buffer, pH 9.0, and then in a microwave oven at 650 W for two cycles of 10 minutes to promote antigenicity. The slides were left to cool at room temperature for at least 20 minutes prior to incubation with goat normal serum (Sigma), further processing for primary antibodies incubation. The primary antibodies were the mono (mAbs) and polyclonal (pAbs), used in serial sections: rabbit pAb anti-collagen type I (Chemicon, Temecula, California), rabbit pAb anti-collagen type III (Chemicon, Temecula, California), rabbit pAb anti-TGF- β 1 (Abcam, Cambridge, UK; ab92486), mouse mAb anti-vimentin (Dako, Glostrup, Denmark, clone V9), and rabbit pAb anti-Factor VIII related antigen (CliniSciences, Guidonia, Italy, Cat# RP012-05). Specific primary antibodies replaced with TBS or nonimmune sera were adopted as negative controls using immunohistochemical procedures. We placed the tissue sections in a wet chamber incubator for one night at 4°C using different primary antibodies, diluted 1:50 in Tris-buffered solution (TBS) with 0.1% crystalline bovine serum albumin (BSA). We detected antibody binding using ABC-peroxidase (Vector Laboratories Inc, Burlingame, California) techniques with 1:200 diluted biotin conjugated goat anti-rabbit immunoglobulin G (Vector Laboratories Incorporated, Burlingame, California) and a 1:200 diluted biotinylated goat anti-mouse immunoglobulin (AO433; DAKO, Glostrup, Denmark), administered as a secondary antibody at room temperature for a 45-minute interval. We generated the enzymatic reaction using 3,1-diaminobenzidine (DAB) (Sigma, St. Louis, Missouri) as a substrate for the ABC-peroxidase procedure, with Meyer hematoxylin as a nuclear counterstain. Immunohistochemical assessment included collagen type I or III predominant expression in defective and healthy sections of tendon tissue, FVIII positive-microvessel neo-formation, expression of TGF- β 1, and the presence of vimentin positive stained fibroblasts, diffused or localized in a perivascular manner across the injured area, indicating potential regeneration/repairment of the CCT, assessed at 100 \times . The scoring of semiquantitative assessment regarding the immunohistochemical reaction in the antigens was as following: 0 (absence of antigen expression), 1 (weak and spotted antigen expression), 2 (weak but profuse antigen expression across the whole specimen), and 3 (profuse and marked antigen expression). The histological and immunohistochemical evaluations were blinded and conducted throughout by two operators, an experienced pathologist and assistant.

2.10 | Real-time PCR array analysis

The RNeasy Mini Kit (Qiagen GmbH, Hilden, Germany) was used for total RNA isolation from biopsies, DNase digestion was performed using the RNase-Free DNase Set (Qiagen). Eight hundred nanograms of total RNA from all specimens was reverse transcribed using an RT2

First Strand kit (Qiagen Sciences, Germantown, Maryland). Real-time PCR was conducted compliant with instructions provided in the Rat Wound Healing RT2 Profiler PCR array (SABiosciences, Frederick, Maryland) employing RT2 SYBR Green ROX FAST Mastermix (SABiosciences).

We performed thermal cycling and fluorescence detection via Rotor-Gene Q 100 (Qiagen), analyzing data with Excel-based PCR Array Data Analysis templates (SABiosciences). We reported the results as an expression of every target gene in the specimens collected at T2 for both groups and compared outcomes to expression of GPDH.

2.11 | Biomechanical analysis

The specimens ($n = 4$) of both groups randomly selected at the beginning of the study were analyzed (T2). The tendon with the attaching calcaneal bone was dissected free from other tissues and removed. They were kept at -70°C until the testing procedure was initiated. Therefore, the distal end of the bone was placed in bone cement and tightly screwed to the machine. The proximal end was cleaned of muscular tissue and then fixed to the testing machine by means of specific metal gripping clamp. The remaining free length of all specimens was adjusted to 6 cm. The total and specific rupture force (N/mm^2) were evaluated using a uniaxial testing machine with analogous documentation facilities (Zwick 7025-3, Zwick, Ulm, Germany). Before measurements were taken, specimens were preloaded for 1 minute with 10 N. The displacement rate was 6 mm/min. Specimens were kept moist throughout the test period with isotonic NaCl solution.

2.12 | Statistical analysis

The sample size was calculated a priori using paired t test, with at least 80% power, alpha-error 0.05 and effect size ($d_z = 0.936421$) obtained from a previous study comparing the hardness percentages (Elax-t% HRD) on elastosonographic evaluation in injured and control tendons.⁶⁸ Power and sample size were analyzed using G-Power software, version 3.1.9.2.

Cardinal data were assessed for normality via the Shapiro-Wilk test. The transversal diameter of the tendon (clinically measured in mm) was examined by paired t test to compare the groups at each time-point. The repeated-measures ANOVA with subsequent Holm-Sidak post hoc test were used to compare the study time-points within each group. Ultrasonographic and Elastosonographic data were not normally distributed; accordingly, all statistical analyses were performed via a nonparametric approach: the Wilcoxon Matched-Pairs Signed Rank Test was adopted to compare the groups at each time point; the Friedman test and subsequent Dunn's multiple comparison test were used to relate study time-points within each group. Histological, immunohistochemical and biomechanical data were compared between groups using the Wilcoxon Matched-pairs Signed Rank Test. A P -value $< .05$ was intended as statistically significant. Data were statistically analyzed with the GraphPad Prism, version 8.2.1 for MacOS (GraphPad Software Inc, San Diego, California).

The mean values for quantitative data were compared, applying the ANOVA test for real-time polymerase chain reaction (RT-PCR) results. *T*-tests were used to determine significant differences ($P < .05$). Repeatability was calculated as the SD of the difference between measurements. All analyses were examined using SPSS 16.0 software (SPSS Inc, Chicago, Illinois) (license of the University of Ferrara, Italy).

3 | RESULTS

3.1 | Clinical evaluation shows improvement in lameness and in tendon thickness in the treated groups

All animals, 24 hours after induction of the lesion showed II-III degree lameness. Over the weeks, regardless of the group, lameness gradually improved and settled at I/II degree 3 weeks after lesion induction. At 4 weeks, a degree of lameness of I degree persisted in both limbs, but at 8 weeks we observed that the animals had loaded the treated pelvic limb, and slightly unloaded the untreated limb which continued to show first degree lameness.

At Ti (healthy tendons) the average mean thickness \pm SD was 8.6 ± 1.1 mm in the treated group, while 8.5 ± 1.2 mm in the control group. At T0 the tendon thickness in the treated group was on average 12.3 ± 1.8 mm, compared with 13.7 ± 2.1 mm in the control group. At T1, the treated group showed an average tendon thickness of 13.1 ± 1.9 mm and in the control group thickness was 14.1 ± 2.0 mm. At T2, the tendon thickness of both groups was on average 9.1 ± 1.4 mm and 9.5 ± 1.7 mm, respectively. No statistical differences between the two groups were observed at any time points ($P > .05$).

We also performed statistical analysis comparing tendon thickness modification in the treated group and in the control group, at four different time points (Ti, T0, T1, T2). The average thickness of the common calcaneal tendon varied considerably both in the treated group ($F = 103.4$; $P < .0001$) and in the control group ($F = 107.1$; $P < .0001$), with a significant increase in the tendon diameter within each group up to T1.

At the end of the study (T2, 8 weeks after treatment) the tendon thickness had decreased significantly compared with T0 ($P < .0001$) and T1 ($P < .0001$) in both groups. However, the treated group revealed no further difference ($P = .1224$) based on the initial healthy tendon condition (Ti), while a statistical difference from Ti to T2 was still observable in the control group ($P = .0297$), as reported in Figure 3A.

3.2 | The B-mode ultrasound evaluation shows a decrease in tendon thickness in the treated group despite lack of valid temporal progression measurement

The B-Mode ultrasound examination conducted at Ti, T0, T1, and T2 highlighted the injuries induced and monitored the repair process.

The areas of the lesion, progressively, at T1 and T2 appeared slightly less hypoechoic, although the examination did not allow for an objective and quantitative assessment of the reparative progression. The results regarding the thickness measurements of the tendons, measured in cross section at the site of the lesion (6 cm from the proximal calcaneal tuberosity) are shown in Figure 3B.

At ultrasound evaluation, no statistical differences were reported in tendon thickness between the two groups at any time point ($P > .05$).

Both groups showed differences on comparison by study time-points within each group (treated group, $Fr = 29.67$, $P < .0001$; control group, $Fr = 29.62$, $P < .0001$).

In the treated group, the tendon thickness increased significantly following the induction of the lesion from Ti (mean \pm SD, 8.4 ± 1.7 mm) to T0 (14.7 ± 2.5 mm, $P = .0012$); the thickness continued to increase significantly up to T1 (15.5 ± 2.4 mm, $P < .0001$), but on study termination (T2) no significant difference was observed (9.7 ± 1.7 mm, $P > .05$) considering the preinjury healthy tendon. The control group showed a similar trend to the treated group in relation to the initial preinjury condition and the other time-points. However, we compared the thickness of the initial injured tendon before treatment (T0) and the end of the study (T2) to the SVF treated tendon and observed that the tendon thickness had decreased significantly ($P = .0071$), in the control group no statistical differences from T0 to T2 were noted ($P = .0855$) (Figure 3B).

3.3 | Elastosonography evaluation shows changes in tendon hardness in the treated group with temporal progression measurement

The hardness percentages (Elax-t%HRD) of the tendons at Ti, T0, T1, and T2 are shown in Figure 3C. In both groups, the hardness percentages (Elax-t%HRD) changed significantly considering the study time-points (treated group, $Fr = 16.30$, $P = .0010$; control group, $Fr = 15.70$, $P = .0013$). On elastosonographic evaluation, the healthy tendon (Ti) possessed significant hard-tendon properties (Figure 4). Fourteen days following lesion induction (T0), the tendons appeared markedly soft. The tendon hardness changed significantly in relation to the condition of the healthy tendon (Ti) and other time-points in both groups.

No significant differences between T0 and subsequent time-points were observed within the groups ($P > .05$), but a dissimilar trend in the two groups during the study was ascertained. At T0, the treated group showed a progressive increase in tendon hardness until completion of the study, while the control group showed an increase in hardness between T0 and T1 and a decrease at the end of the study (T2) reaching an average tendon hardness percentage that was lower than T0. No significant differences were observed comparing the two groups at Ti ($P = .8501$), T0 ($P = .6221$) and T1 ($P = .5693$). However, at T2, a significant recovery of hardness was observed in the treated group compared with the control ($W = -54.0$; $P = .0342$).

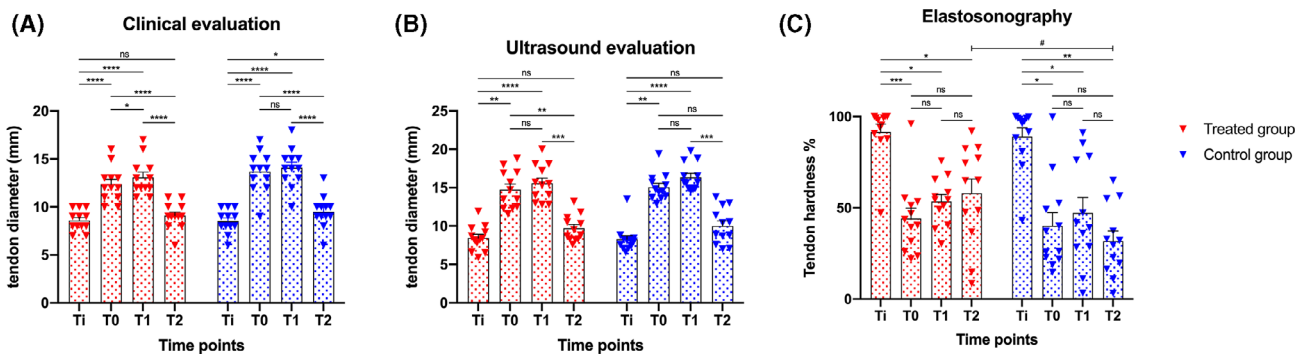


FIGURE 3 A, Tendon diameter clinically measured in treated group and control group at each time point, expressed in millimeters (mm). B, Tendon diameter (mm) echographically measured in treated group and control group at each time point. C, Tendon hardness (%) at elastosonographical evaluation in both groups at each time point. Red and blue triangles indicate the single measurements scattered in groups; boxes indicate mean values; bars indicate standard errors; Ti: initial healthy tendon condition immediately before induction of experimental tendon lesion; T0: 14 days after the induction of tendon lesion (treated group underwent therapy with stromal vascular fraction); T1: 4 weeks after T0; T2: end of the study, 8 weeks after T0. *P*-values, ns: not significant; **P* < .05; ***P* < .01; ****P* < .001; *****P* < .0001; # indicates the only significant difference (*P* < .0342) found between groups

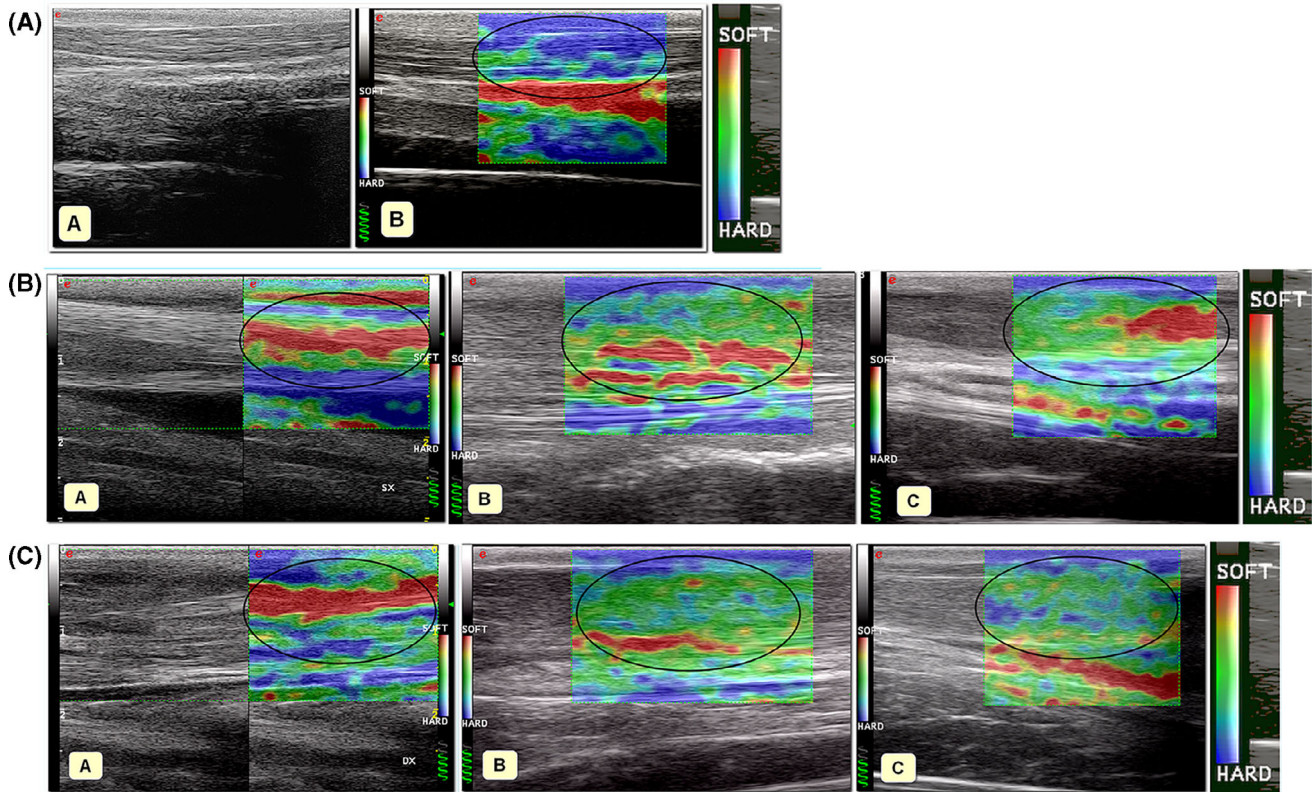


FIGURE 4 A, B-mode (A) and sonoelastographic (B) appearance of the normal CCT. Normal CCT is mostly hard, which is represented in color-coded map in blue (encircled in black); B, B-mode and sonoelastographic features of CCT 15 days after the iatrogenic lesion in a subject of non-treated group (A). The elastogram of CCT was mostly red (soft). The same tendon at 1-month follow-up (B) and 2-month follow-up (C): the elastogram was mostly green (intermediate elastographic features) with areas of red (softness, encircled in black). C, B-mode and sonoelastographic features of the CCT 15 days after the iatrogenic lesion in a subject of treated group (A). The elastogram was mostly red (soft areas, encircled in black). The elastogram of the same tendon at 1-month follow-up (B) was mostly green (intermediate elastographic features, encircled in black). The elastogram of the same tendon at 2-months follow-up (C) was green (intermediate sonoelastographic features) with several areas of blue (areas of hardness, encircled in black)

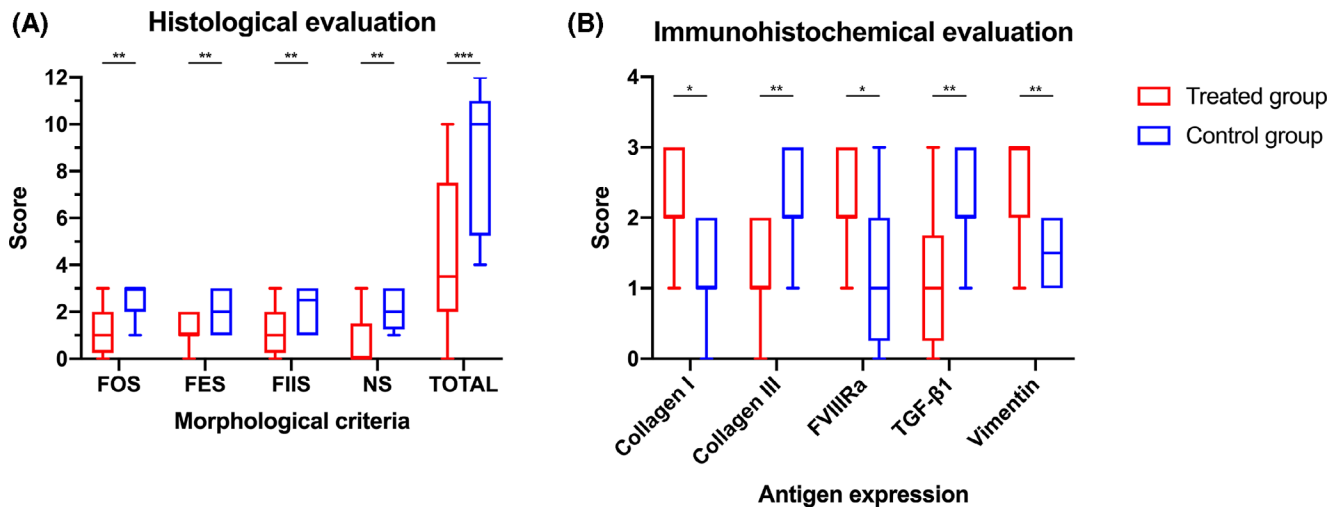


FIGURE 5 A, Histological score of excised tendons at the end of the study (T2) in treated group and control group. FOS: fiber orientation score; FES: fiber edema score; FIIS: infiltrative-inflammatory score; NS: necrosis score; TOTAL: total score; B, Immunohistochemical score of excised tendons at the end of the study (T2) in treated group and in control group. The ends of the whiskers show minimum and maximum score values; boxes show the median, the first and the third quartile; *P*-values, ns: not significant; **P* < .05; ***P* < .01; ****P* < .001; *****P* < .0001

3.4 | Histological analysis shows an improvement of FOS, FES, FIIS, and NS parameters in the treated groups

Morphological and histological scores were evaluated for each sample at T2 demonstrating that the FOS, FES, FIIS, and NS parameters were generally improved in tendons pertaining to the treated group, compared with the untreated controls. In particular, in the treated group, the average score of FOS, FES, FIIS and NS was 4.3 ± 3.3 , while in the untreated group the score was 8.8 ± 2.9 . A significant overall difference between the degree of tissue repair in the treated group, compared with the untreated group, was evident from the statistical analysis ($W = 66.0$; $P = .0010$). Comparing the same areas in CCT tendons, the treated group displayed a longitudinal pattern of the fibers revealing improved alignment and less damage (FOS—treated group: 1.2 ± 1.1 ; control group: 2.5 ± 0.7 ; $W = 45.0$; $P = .0039$), as well as the parameters related to the presence of necrosis (NS, treated group: 0.7 ± 1.2 ; control group: 2.1 ± 0.8 ; $W = 55.0$; $P = .0020$), the inflammatory infiltrative process (FIIS—treated group: 1.3 ± 1.0 ; control group: 2.2 ± 0.9 ; $W = 36.0$; $P = .0078$) and the presence of edema / myxoid aspect (FES—treated group: 1.2 ± 0.7 ; control group: 2.0 ± 0.8 ; $W = 36.0$; $P = .0078$). In general, all parameters were significantly lower ($P < .5$) in the treated group compared with control (Figure 5A).

3.5 | Immunohistochemical analysis shows high expression of COL1, FVIII, and significantly low expression of COL3 in the treated groups

Immunohistochemical results revealed significant differences in all evaluated antigens in the tendons belonging to the SVF treated group

compared with the untreated controls. Regarding collagen expression, the average score of treated animals was 2.3 ± 0.6 relative to 1.2 ± 0.7 observed in the untreated tendons ($W = -42.0$; $P = .017$). Conversely, COL3 was overexpressed in the control group (average 2.3 ± 0.6 relative to 1.3 ± 0.6 observed in the SVF treated group; $W = 56.0$; $P = .0098$) indicating, at T2, a fibrous scarring tissue formation in the lesion area. These results displayed the same trend expressed by TGFβ1, overexpressed in the fibroblasts and inflammatory cells of the control group (average 2.2 ± 0.7) compared with the SVF treated tendons (1.1 ± 0.9) ($W = 36.0$; $P = .0078$). In the treated group, the presence of a less fibrous and more remodeling activity was also characterized by a more active neo-angiogenesis, indicated by a greater expression of FVIII (av. 2.3 ± 0.6) than the average expression observed in the control tendons (1.2 ± 0.9) ($W = -59.0$; $P = .0161$). (Figure 5B). These results were also observed at lower power magnifications, in the stained histological sections using the histochemical Herovici method. In the treated group at T2, these sections clearly provided younger connective tissue (colored in blue or light blue) in combination with a more mature and organized collagen tissue (red in color). The control group, however, concurrently displayed a still modified central lesion with hypoxic phenomena and tissue necrosis, appearing yellow/orange in color. The connective tissue seemed notably mature and organized in a mature fibrous-scar tissue, bright red in color around most of the central—yellow area (Figure 6).

3.6 | Gene expression shows a high expression of COL1, VEGF, and a significant decrease in MMP1m COL3 and sclerodermin genes

Gene expression related to the gene of tenogenesis and tendon regeneration shows that AAMG products contain a high expression of

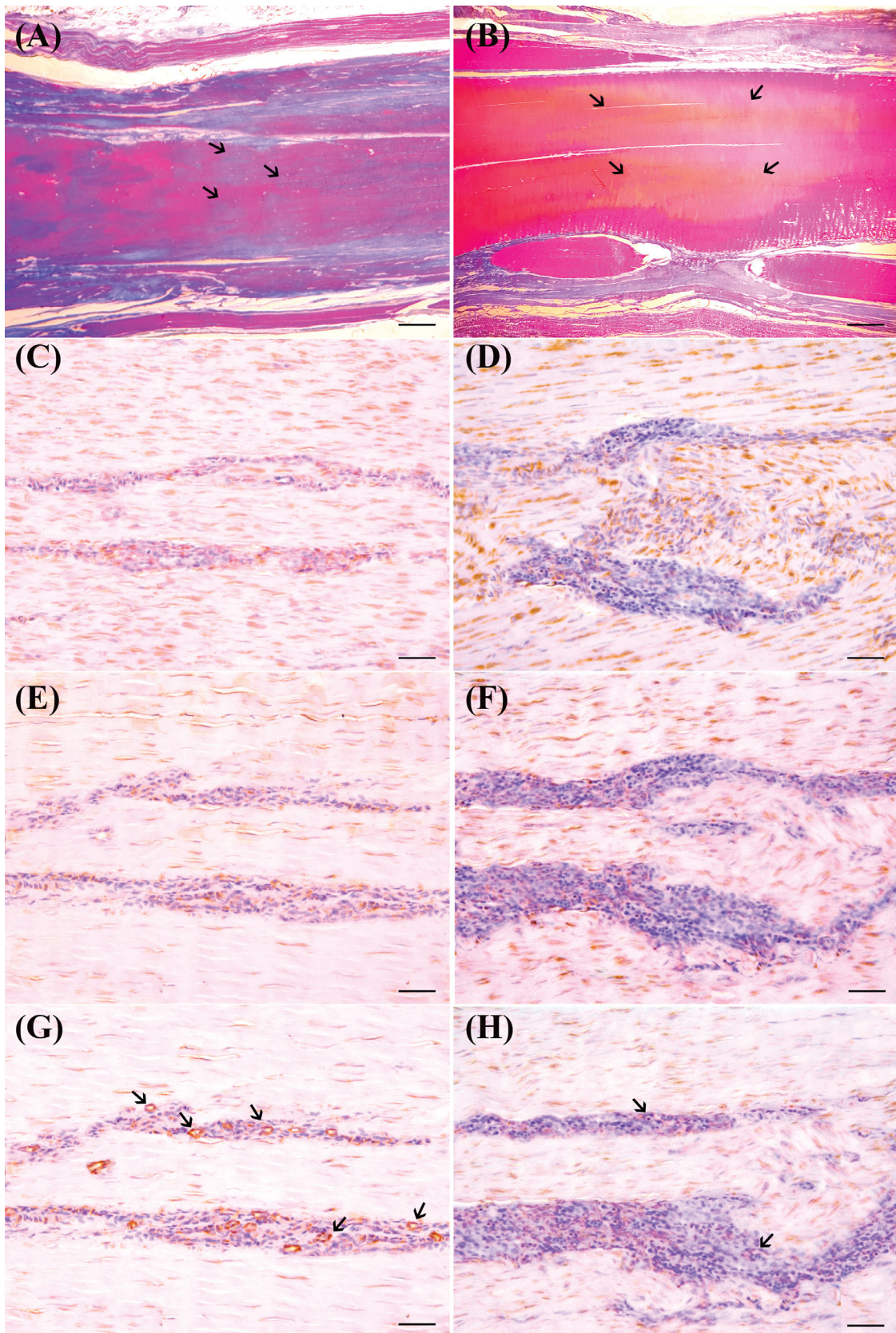


FIGURE 6 Legend on next page.

COL1, crucial to the structural organization of the tendon VEGF and to angiogenesis. Moreover, we observed an evident reduction on metalloprotease expression (mainly MMP1) and on collagen type 3 (COL3), and sclerodermin genes that are typical of scars. As regards epigenetic changes, we further noted that the miRNA related to tendinogenesis in AAMG-derived products was up-expressed compared with the control group. Specifically stromal contribution induced an increase on miRNA205, miRNA 145-5, miRNA 100, miRNA 195, and let-7 related to tendon healing primarily during effective angiogenesis and a reduction in miRNA29 was associated to the presence of injury (Figure 7).

3.7 | Biomechanical analysis

As for biomechanical analysis, the specific rupture force and the total rupture force were considered. The mean specific rupture force was 28.3 N/mm² in the treated group and 27.8 N/mm² in the control group ($P = .79$). The total rupture force at T2 was 10.2 kN in the treated group and 9.87 kN in the control. The difference was not statistically significant ($P = .89$).

4 | DISCUSSION

This study showed that the injection of SVF from AAMG, provided a significant clinical improvement in terms of lameness relief and function restoration. Our results highlighted an important difference between the reparative and regenerative process established in treated tendons compared with untreated tendons, suggesting an effective regenerative capacity induced by the use of SVF in treating tendinopathies. The use of SVF will accordingly modulate the inflammatory process directing a possible transition from pro-inflammatory and pro-fibrotic to a pro-regenerative cellular response, providing thus a reduction in inflammatory cell infiltration and an organized placement of ECM elements.^{69,70}

To date, studies on the regenerative effects of adipose SVF obtained by mechanical disruption in tendon lesions are still limited.

This is the first study, on an animal model employing a mechanical fat breakdown system (Rigenera system) as an alternative to enzymatic digestion.⁵⁹⁻⁶² The product obtained from the mechanical digestion of ovine fat was characterized by a well-preserved vascular/stromal organization with perivascular integrity. Flow cytometry analysis of SVF showed expression of specific mesenchymal stromal stem cell markers (CD34, CD105, CD90, CD73, CD117), noted in previous literature^{53,71-74} by enzymatic digestion.

Our study revealed that the use of 500 UI of collagenase type IA1 was a feasible and effective dose for the induction of iatrogenic tendon injury in animal models (ovine) as reported in literature.⁷⁵ We reported no cases of tendon rupture and the iatrogenic lesion induced by collagenase possessed similar features to spontaneous tendon injuries such as hypercellularity, hypervascularity, loosening of ECM organization and an increased vascularization. These findings are analogous to those found in tendinopathies of spontaneous origin.⁷⁶

In this study, tendons treated with SVF from AAMG showed a structure that was stackable to normal tendons in terms of thickness and stiffness (hardness), compared with untreated group.

Indeed, tendon diameter at T1 in treated and control group was 8.6 ± 1.1 and 8.5 ± 1.2 while in T2 was 9.1 ± 1.4 and 9.5 ± 1.7 respectively and the difference was significant in control group.

Moreover, at T2 a significantly recovery hardness was found in treated group (62%) compared with control group (32%).

In contrast with our findings, Geburek and coworkers⁷⁷ in their surgical induced lesion in equine tendons in sonographic and ultrasonographic evaluation, did not found statistical differences between control and treated group at same time point (total cross-sectional area under 800 mm² at final endpoint). Moreover, Uselli et al⁶³ use ultrasound (US) in their study on human treated for Achilles' tendinopathy to make a comparison between PRP and SVF (initial tendon diameter 8.93 ± 2.1 and 10.7 ± 3.3 respectively and 8.6 ± 2.0 and 10.4 ± 3.3 at final follow-up). Authors conclude US were a useful, reliable tool to identify tendon pathology and lesion site but did not allow for any relevant information regarding the lesion evolution during the follow-up.

On the contrary we believe that the association between classical b-mode and elastosonography are a valid tool to evidence tendinopathy evolution. This finding supports the hypothesis that SVF

FIGURE 6 Tissues sections obtained from sheep CCT, after induction of collagenase type I iatrogenic lesions, injected or not with SFV cells, and sampled 8 weeks after therapy. Tendons stained with Herovici polychrome stain, highlight the longitudinal orientation of collagen fibers after transplantation of SFV cells, without necrotic and/or edematous aspect (A, scale bar = 13.3 μm); note that, in central area of the treated tendon, not completely mature, and longitudinal configured collagen fibers, identified as blue stained fibers admixed with red ones. In the control tendon (B, scale bar = 13.3 μm), Herovici stain shows the presence of mature and longitudinally oriented collagen fibers (ie, predominantly strong Herovici red stained fibers in tendon sections) at the periphery of the collagenase injected area (arrows). In the central part of CCT, lesion (stained in yellowish–orange) is surrounded by completely mature, and fingerprint configured collagen fibers, identified as red stained fibers without pre-collagen admixed blue fibers. Immunohistochemistry stains for collagen type I (CI), and collagen type III (CIII) show a high expression of CI (C, scale bar = 250 μm) and a very low expression of CIII (E, scale bar = 250 μm) in SVF cells–treated tendon. On the contrary, an opposite trend is observed in untreated control tendon in which a low expression of CI (D, scale bar = 250 μm), and high expression of CIII (F, scale bar = 250 μm) are observed. IHC stains for FVIIIIRa reveal a large number of small and medium sized positive–micro-vessels, in SVF cells–treated CCT (arrows) (G, scale bar = 250 μm). Although some rare endothelial cells are positive, a substantial absence of neo-angiogenesis is observed in the control tendon, where only the presence of some small capillaries is sporadically observed (H, scale bar = 250 μm)

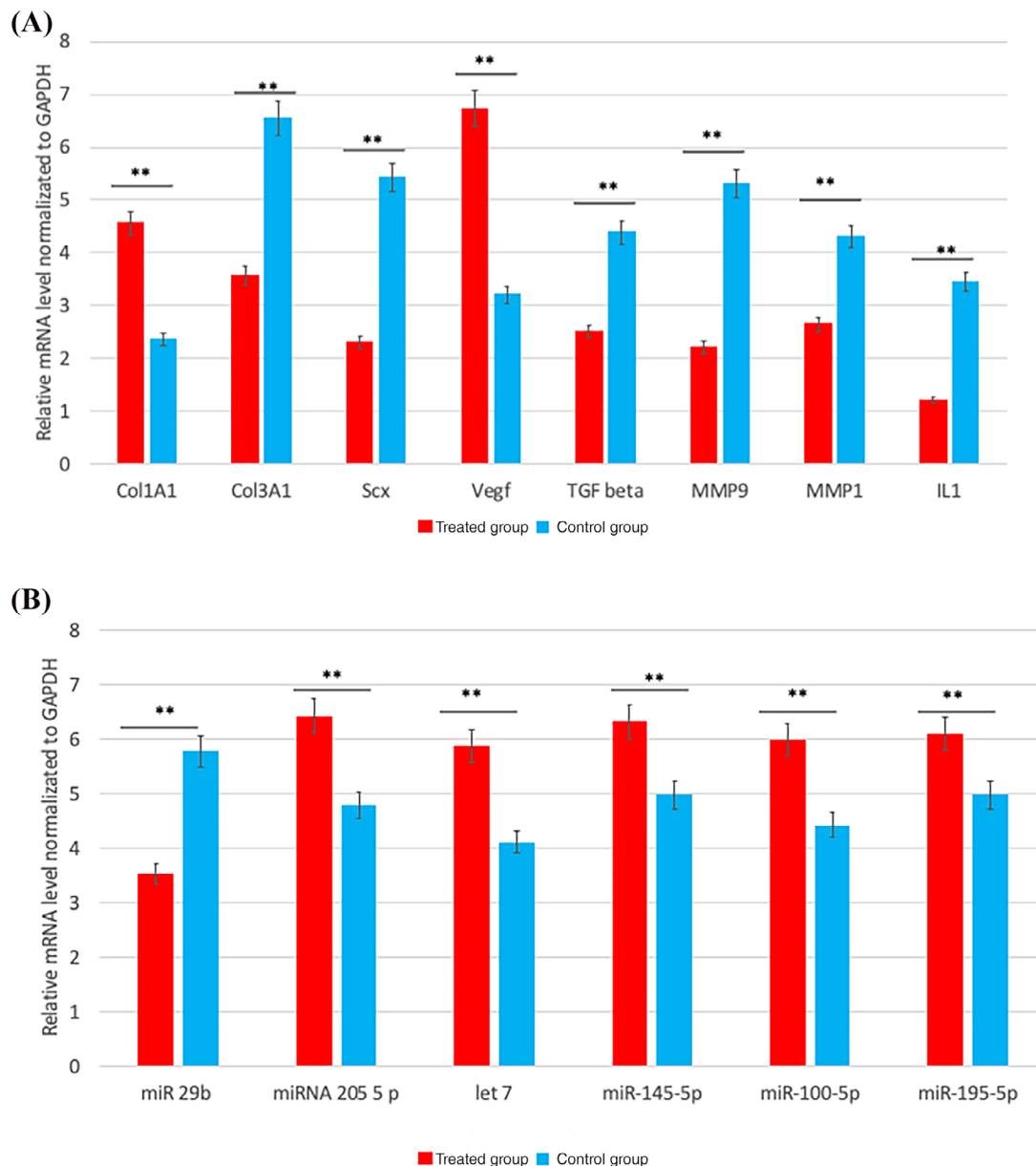


FIGURE 7 Semiquantitative analyses of gene expression of Col1a1 (collagen type I), Col3a1 (collagen type III), Scx (sclerodermin) Vegf (vascular endothelial growth factor); TGF beta (transforming growth factor), Mmp1 (metalloproteinase 1), Mmp9, interleukin 1 (IL1), miRNA group involved on xenogenesis such as miR 29b, miRNA 205 5 p, let 7, miR-145-5p miR-100-5p, miR-195-5p in treated (group A in red), and no treated (group b in blue) group. Data were quantified and normalized by using the quantitative real-time polymerase chain reaction (RT-qPCR) procedure. Each bar represents the fold change (FC) SD of the normalized values. Repeated-measures ANOVA with a post hoc analysis using Bonferroni's multiple comparison. *T* tests were used to determine significant differences ($P = .05$). * $P = .05$; ** $P = .01$; *** $P = .001$. Repeatability was calculated as the SD of the difference between measurements

administration promotes healing of the tendon and may induce restoration of original tendon structure and morphology.

Improvements were also observed in tendon morphology compared with treatment without SVF.

The significant improvement in morphologic scores for tendon organization (total morphological score of FOS, FES, FIIS and NS was 4.3 ± 3.3 , while in the untreated group the score was 8.8 ± 2.9 .) is not attributable to the tendon matrix composition, but rather to maturation and remodeling of the existing collagen. Furthermore, the

architecture of the remodeled tissue itself is relevant to the mechanical properties of the tendon, which enables resistance to repetitive strains without recurrences of injury. Similar results were found by Behfar and coworkers⁵⁸ in their study on injured flexor tendon in rabbits, demonstrated that SVF-injected tendons exhibited more organized neotendon characterized by parallel or linear orientation of collagen bundles and superior fibrillar continuity in treatments over controls (46.45 ± 6.39 ; 27.99 ± 5.79 and 62.91 ± 3.98 ; 46.99 ± 4.13 , respectively). Oshita and coworkers⁴⁴ showed that ASC group

exhibited decreased levels of disrupted collagen fibers, cellularity, and hypervascularity with significantly lower degree of tendon degeneration than the control group at both time points (the median Bonar scale was 2.5 and 5.33, respectively 4 weeks after treatment, and 1 and 4 respectively 12 weeks after treatment).

Therefore, Chen et al⁷⁸ in their study on rotator cuff tears in rats, had similar results. Histological analysis reveal that collagen fibers were neater and more parallel in the hADSC-injected rats at day 7, with no difference in at final follow-up (descriptive analysis).

On the contrary, Geburek et al⁷⁷ reveal no significant differences between treated and untreated group with respect to total scores, scores for fiber arrangement, scores for metabolic activity and sub-scores for fiber structure and alignment, morphology of tenocyte nuclei, variations in cell density or vascularization (total Aström and Rausing score 43 vs 39).

Our findings, together with the improved tendon architecture suggest the ability of adipose-derived adult stem cells to ameliorate the regenerative capacity of tendon healing. Moreover, both elastosonographic and histological results are completely concordant herein.

This affirmation is supported also by the immunohistochemical results effectively showing regenerative factors (collagen I, FVIII, vimentin) that were significantly higher in the treated group (COL1 was 2.3 ± 0.6 vs 1.2 ± 0.7 ; FVIII was 2.3 ± 0.6 vs 1.2 ± 0.9 ; Vimentin was 2.2 ± 0.7 vs 1.5 ± 0.7). Although, scarring and fibrotic factors (collagen III, TGF- β 1) were significantly higher in the control group (COL3 was 2.3 ± 0.6 vs 1.3 ± 0.6 ; TGF β 1 was 2.2 ± 0.7 vs 1.1 ± 0.9).

These results reveal a dominant anti-inflammatory and immunosuppressive impact on these cells.^{79,80} According to our findings, Oshita et al⁴⁴ showed the area positively stained for type I collagen increased over time in the ASC group. The area positively stained for type III collagen decreased over time in the ASC group (descriptive analysis).

Behfar et al⁵⁸ showed an increased expression of Col I in SVF-treated tendons, which was statistically significant as compared with controls (median and interquartile range value 3.00 (2.00-3.00) vs 1.00 (0.75-2.00) Even Lu et al⁶¹ evaluates tendon healing in rotator cuff tendinopathy in rat. They showed that the expression level of collagen I in the SVF-FG treatment group was obviously higher than the expression in the control group (type I collagen/type III collagen area ratio 1.69 ± 0.43 vs 1.31 ± 0.34 , $P = .031$). Consistently, the expression level of collagen III in the SVF-FG treatment group was slightly higher than the expression in the control group.

Uysal et al⁸¹ analyzed Achilles' tendon healing in rabbits. The anti-TGF- β 1, 2, 3 antibody immunohistochemical stainings were found out to be statistically lower in the experimental group when compared with the values of the control group (anti-TGF- β 1 was 22.23 ± 3.88 vs 33.84 ± 3.67 ; anti-TGF- β 2 24.69 ± 3.87 vs 35.96 ± 4.64 ; the anti-TGF- β 3 values 28.81 ± 4.02 vs 39.56 ± 4.74 , respectively). On the contrary Mora et al⁸² evaluating tendon cuff repair in rats, showed there were no differences in the amount of collagen type I and collagen type III at either time points of their work. In the untreated group, collagen fibers were detected at 1 week, whereas in

the ASCs group, fibers were not clearly detectable until the last sacrifice time point (descriptive analysis).

Treatment with mesenchymal stem/stromal cells have indeed demonstrated efficiency in mitigating fibrosis in various applications and has aroused noteworthy interest in the scientific field. In this study, moreover, we demonstrate that SVF treatment is able to increase the expression of FVIIIa, an angiogenic related factor, crucial in tissue healing.

This paracrine effect has been reported in other wound healing studies. Our study revealed that tenocytes, upon inflammatory trigger/stimuli, tend to express inflammatory cytokines, including, interleukin (IL)-1 β (relative mRNA level normalized to GAPDH 3.5 vs 1.2) and (TGF)- β (relative mRNA level normalized to GAPDH 4.3 vs 2.5).

Several miRNAs seem to be involved in tendon inflammation, including microRNA (miR)-29b which is implicated in the regulation of IL-33-mediated inflammation and is considered a negative regulation of tenogenesis (relative mRNA level normalized to GAPDH 5.8 vs 3.4). By contrast, miR-205 is related to VRGF synthesis. Expression of miRNAs associated with tendon regeneration such as miR-145, miR-100, miR-195, and let-7 were observed in our studies.

According to our results, Viganò' and coworkers⁸³ showed that coculture with ADSC not only reduced the expression of fibrosis and catabolic markers but it also enhanced the production of cytokines and growth factors able to counteract the inflammatory process and to contribute to tissue regeneration such as reduce the expression of collagen type III and metalloproteases-1 in a significant manner (57% and 41%, respectively), and at the same time, it enhanced the production of VEGF, IL-1Ra, and IL 6.

Several studies have suggested the concept of the "vicious circle" in tendon wound healing which causes prolonged symptoms of tendinopathy and in particular, Oshita and colleagues⁴⁴ claimed that ASC administration improved degeneration in tendinopathy through a positive ECM turnover with normalization of collagen ratio. The main difference between our study and Oshita's analysis is the use of mechanical digestion which enabled the SVF to neutralize the "vicious circle" and enzymatic digestion. Furthermore, Costa-Almeida and colleagues demonstrated that ASCs were able to improve COL1/COL3 ratio, suggesting a role in modulating the microenvironment of tendon niche in vitro, as well as improving tendon healing in vivo.⁸⁴

Some authors, namely de Girolamo et al have reported noteworthy results in clinical trials regarding patients affected by tendon injury, demonstrating safety, and efficacy of treatments with SVF in clinical recovery compared with conventional treatments.⁸⁵ Furthermore, Ferracini and colleagues⁸⁶ used microfragmented adipose tissue in eight patients with tendon rupture and documented a decrease in peritendinous reaction with a biological activation of intraslesional fiber deposition and orientation; however, the triggering mechanism still remains unclear. Future experiments are required to examine the expression of specific miRNAs in the healing time points to define the specific regulating mechanisms. The epigenetic regulation of gene expression has been determined in mammalian systems, including sheep. Inflammation is a generalized occurrence associated with all tendinopathies. However, the sustained disorganization of ECM

increases the risk of tendon damage recurrence. It is noteworthy to recall the potential for epigenetic regulation in the expression of inflammatory genes, as well as the genes associated with tendon repair. Additionally, extrapolation of the epigenetic changes in inflammation may provide a better understanding of tendons.

Even if in our study no differences in specific and total rupture force were observed in biomechanical analysis (28.3 N/mm² the treated group vs 27.8 N/mm² in the control group; total rupture force was 10.2 kN vs 9.87 kN), in literature several studies^{59,78,81,87} demonstrate better biomechanical results in tendon treated with AAMG and SVF compared with control groups (eg, s in Behfar study, ultimate stress was 18.92 ± 1.49 N/mm² vs 4.7 ± 2.48 N/mm²).

Therefore, we can conclude our findings are related to the very limited sample size.

5 | CONCLUSION

Our findings suggest that the beneficial effects of tendon repair, induced by SVF, is attributable to the maintenance and induction of tendon fiber organization rather than to the increase in a pool of cells as part of the healing process. Moreover, our approach further strengthens the rationale that broad anti-inflammatory and immunomodulatory features in molecules released by cells in the SVF may be efficient in treating tendon diseases and may be a relevant alternative to traditional anti-inflammatory therapies (NSAIDs and FAS). In conclusion, our study affirms that, at 2-month post inoculation, the repairing process of the tendons treated with implantation of cells originating from the vascular-stromal fraction yielded more satisfactory outcomes compared with results observed in untreated tendons, both in terms of tendon rigidity, evaluated in elastosonography, and from a histological, immunohistochemical perspective. Additionally, we observed positive effects in matrix composition in the treated tendons, and in collagen deposits as well as noting improved neoangiogenesis within the lesion sites.

ACKNOWLEDGMENT

The authors are grateful to Dr. Giuseppina Caraglia, University of Naples "Vanvitelli", for careful revision of the manuscript.

CONFLICT OF INTEREST

The authors declared no potential conflicts of interest.

AUTHOR CONTRIBUTIONS

A.P.P.: conception and design, collection and/or assembly data, manuscript writing; V.R., L.P., R.B., G.R., L.G., C.M., B.Z.: collection and/or assembly data, data analysis and interpretation; L.S. and A.V.: ultrasound and elastosonographic investigations, data analysis and interpretation; A.M.T.: statistical analysis; C.V.: collection of data, anesthetic procedures, animal assessment; A.G.: conception and design; F.D.F.: collection and/or assembly data, data analysis and interpretation, manuscript writing, final approval of manuscript.

DATA AVAILABILITY STATEMENT

The datasets generated during and/or analyzed during the current study are available from the corresponding author upon reasonable request.

ETHICS STATEMENT

The present study was approved by the Italian Ministry of Health (authorization number 620/2018-PR).

ORCID

Angela Palumbo Piccionello  <https://orcid.org/0000-0003-4076-4729>

Adolfo Maria Tambella  <https://orcid.org/0000-0002-6590-1876>

Livio Galosi  <https://orcid.org/0000-0001-5094-8359>

Antonio Gigante  <https://orcid.org/0000-0003-0772-563X>

Barbara Zavan  <https://orcid.org/0000-0002-4779-4456>

Francesco De Francesco  <https://orcid.org/0000-0003-2977-7828>

Michele Riccio  <https://orcid.org/0000-0001-5554-4759>

REFERENCES

- Zumwalt M, Reddy AP. Stem cells for treatment of musculoskeletal conditions orthopedic/sports medicine applications. *Biochim Biophys Acta Mol Basis Dis.* 1866;2020:165624.
- WHO Study on Global Ageing and Adult Health (SAGE). WHO Report; August 9, 2019.
- Walden G, Liao X, Donell S, et al. A clinical, biological, and biomaterials perspective into tendon injuries and regeneration. *Tissue Eng Part B Rev.* 2017;3:44-58.
- Abraham AC, Shah SA, Golman M, et al. Targeting the NF-κB signaling pathway in chronic tendon disease. *Sci Transl Med.* 2019;11:eaav4319.
- Kane SF, Olewinski LH, Tamminga KS. Management of Chronic tendon injuries. *Am Fam Physician.* 2019;100:147-157.
- Fitzpatrick J, Bulsara M, Zheng MH. The effectiveness of platelet-rich plasma in the treatment of tendinopathy: a meta-analysis of randomized controlled clinical trials. *Am J Sports Med.* 2017;45:226-233.
- Kujala UM, Sarna S, Kaprio J. Cumulative incidence of Achilles tendon rupture and tendinopathy in male former elite athletes. *Clin J Sport Med.* 2005;15:133-135.
- Longo UG, Ronga M, Maffulli N. Achilles tendinopathy. *Sports Med Arthrosc Rev.* 2018;26(1):16-30. <https://doi.org/10.1097/JSA.000000000000185>
- Gross CE, Lampley A, Green CL, et al. The effect of obesity on functional outcomes and complications in total ankle arthroplasty. *Foot Ankle Int.* 2016;37:137-141.
- Magnan B, Bondi M, Pierantoni S, et al. The pathogenesis of Achilles tendinopathy: a systematic review. *Foot Ankle Surg.* 2014;20(3):154-159.
- Jomaa G, Kwan CK, Fu SC, et al. A systematic review of inflammatory cells and markers in human tendinopathy. *BMC Musculoskelet Disord.* 2020;21(1):78.
- Galatz LM, Gerstenfeld L, Heber-Katz E, et al. Tendon regeneration and scar formation: the concept of scarless healing. *J Orthop Res.* 2015;33(6):823-831.
- Frankewycz B, Penz A, Weber J, et al. Achilles tendon elastic properties remain decreased in long term after rupture. *Knee Surg Sports Traumatol Arthrosc.* 2018;26(7):2080-2087.
- Childress MA, Beutler A. Management of chronic tendon injuries. *Am Fam Physician.* 2013;87(7):486-490.

15. Gerdesmeyer L, Mittermayr R, Fuerst M, et al. Current evidence of extracorporeal shock wave therapy in chronic Achilles tendinopathy. *Int J Surg*. 2015;24(pt B):154-159.
16. Bannuru RR, Flavin NE, Vaysbrot E, et al. High-energy extracorporeal shock-wave therapy for treating chronic calcific tendinitis of the shoulder: a systematic review. *Ann Intern Med*. 2014;160(8):542-549.
17. Couppé C, Svensson RB, Silbernagel KG, et al. Eccentric or concentric exercises for the treatment of tendinopathies? *J Orthop Sports Phys Ther*. 2015;45(11):853-863.
18. Barker-Davies RM, Nicol A, McCurdie I, et al. Study protocol: a double blind randomised control trial of high volume image guided injections in Achilles and patellar tendinopathy in a young active population. *BMC Musculoskelet Disord*. 2017;18(1):204.
19. Chaudhry FA. Effectiveness of dry needling and high-volume image-guided injection in the management of chronic mid-portion Achilles tendinopathy in adult population: a literature review. *Eur J Orthop Surg Traumatol*. 2017;27(4):441-448.
20. Brockmeyer M, Diehl N, Schmitt C, et al. Results of surgical treatment of chronic patellar tendinosis (Jumper's knee): a systematic review of the literature. *Arthroscopy*. 2015;31(12):2424-9.e3.
21. Ahmad Z, Siddiqui N, Malik SS, et al. Lateral epicondylitis: a review of pathology and management. *Bone Joint J*. 2013;95-B(9):1158-1164.
22. Baltes TPA, Zwiers R, Wiegerinck JJ, et al. Surgical treatment for midportion Achilles tendinopathy: a systematic review. *Knee Surg Sports Traumatol Arthrosc*. 2017;25(6):1817-1838.
23. Shapiro E, Grande D, Drakos M. Biologics in Achilles tendon healing and repair: a review. *Curr Rev Musculoskelet Med*. 2015;8(1):9-17.
24. Hart L. Corticosteroid and other injections in the management of tendinopathies: a review. *Clin J Sport Med*. 2011;21(6):540-541.
25. Aicale R, Bisaccia RD, Oliviero A, et al. Current pharmacological approaches to the treatment of tendinopathy. *Expert Opin Pharmacother*. 2020;21(12):1467-1477.
26. Dilger CP, Chimenti RL. Nonsurgical treatment options for insertional Achilles tendinopathy. *Foot Ankle Clin*. 2019;24(3):505-513.
27. Chen C, Hunt KJ. Open reconstructive strategies for chronic Achilles tendon ruptures. *Foot Ankle Clin*. 2019;24(3):425-437.
28. Bottagisio M, D'Arrigo D, Talò G, et al. Achilles tendon repair by Decellularized and engineered xenografts in a rabbit model. *Stem Cells Int*. 2019;2019:5267479.
29. Rinoldi C, Fallahi A, Yazdi IK, et al. Mechanical and biochemical stimulation of 3D multilayered scaffolds for tendon tissue engineering. *ACS Biomater Sci Eng*. 2019;5(6):2953-2964.
30. Soroceanu A, Sidhwa F, Aarabi S, et al. Surgical versus nonsurgical treatment of acute Achilles tendon rupture: a meta-analysis of randomized trials. *J Bone Joint Surg Am*. 2012;94(23):2136-2143.
31. Sebbag E, Felten R, Sagez F, et al. The world-wide burden of musculoskeletal diseases: a systematic analysis of the World Health Organization burden of Diseases database. *Ann Rheum Dis*. 2019;78:844-848.
32. Safiri S, Kolahi AA, Smith E, et al. Global, regional and national burden of osteoarthritis 1990-2017: a systematic analysis of the Global Burden of Disease Study 2017. *Ann Rheum Dis*. 2020;79:819-828.
33. Greising SM, Corona BT, Call JA. Musculoskeletal regeneration, rehabilitation, and plasticity following traumatic injury. *Int J Sports Med*. 2020;41:495-504.
34. Gaspar D, Spanoudes K, Holladay C, et al. Progress in cell-based therapies for tendon repair. *Adv Drug Deliv Rev*. 2015;84:240-256.
35. Kaux JK, Crielgaard JM. Platelet-rich plasma application in the management of chronic tendinopathies. *Acta Orthop Belg*. 2013;79:10-15.
36. Filardo G, Di Matteo B, Kon E, et al. Platelet-rich plasma in tendon-related disorders: results and indications. *Knee Surg Sports Traumatol Arthrosc*. 2018;26:1984-1999.
37. Tang JB, Zhou YL, Wu YF, et al. Gene therapy strategies to improve strength and quality of flexor tendon healing. *Expert Opin Biol Ther*. 2016;16:291-301.
38. Freedman BR, Mooney DJ. Biomaterials to mimic and heal connective tissues. *Adv Mater*. 2019;31:e1806695.
39. De Francesco F, Ricci G, D'Andrea F, et al. Human adipose stem cells: from bench to bedside. *Tissue Eng Part B Rev*. 2015;21:572-584.
40. De Francesco F. Editorial: mesenchymal stem cells and interactions with scaffolds—biomaterials in regenerative medicine: from research to translational applications. *Front Cell Dev Biol*. 2019;7:193.
41. Indino C, D'Ambrosi R, Usulli FG. Biologics in the treatment of Achilles tendon pathologies. *Foot Ankle Clin*. 2019;24:471-493.
42. Jo CH, Chai JW, Jeong EC, et al. Intratendinous injection of autologous adipose tissue-derived mesenchymal stem cells for the treatment of rotator cuff disease: a first-in-human trial. *STEM CELLS*. 2018;36(9):1441-1450.
43. Usulli FG, D'Ambrosi R, Maccario C, et al. Adipose-derived stem cells in orthopaedic pathologies. *Br Med Bull*. 2017;124:31-54.
44. Oshita T, Tobita M, Tajima S, et al. Adipose-derived stem cells improve collagenase-induced tendinopathy in a rat model. *Am J Sports Med*. 2016;44:1983-1989.
45. Lee SY, Kwon B, Lee K, et al. Therapeutic mechanisms of human adipose-derived mesenchymal stem cells in a rat tendon injury model. *Am J Sports Med*. 2017;45:1429-1439.
46. Kemilew J, Sobczyńska-Rak A, Żylińska B, et al. The use of allogenic stromal vascular fraction (SVF) cells in degenerative joint disease of the spine in dogs. *In Vivo*. 2019;33(4):1109-1117.
47. Shen H, Kormpakis I, Havlioglu N, et al. The effect of mesenchymal stromal cell sheets on the inflammatory stage of flexor tendon healing. *Stem Cell Res Ther*. 2016;7:144.
48. De Francesco F, Mannucci S, Conti G, et al. A non-enzymatic method to obtain a fat tissue derivative highly enriched in adipose stem cells (ASCs) from human lipoaspirates: preliminary results. *Int J Mol Sci*. 2018;19:2061.
49. Dai Prè E, Busato A, Mannucci S, et al. In vitro characterization of adipose stem cells non-enzymatically extracted from the thigh and abdomen. *Int J Mol Sci*. 2020;21:3081.
50. Aronowitz JA, Lockhart RA, Hakakian CS. Mechanical versus enzymatic isolation of stromal vascular fraction cells from adipose tissue. *Springerplus*. 2015;4:713.
51. Andia I, Maffulli N, Burgos-Alonso N. Stromal vascular fraction technologies and clinical applications. *Expert Opin Biol Ther*. 2019;19:1289-1305.
52. Bertheuil N, Chaput B, Ménard C, et al. Adipose mesenchymal stromal cells: definition, immunomodulatory properties, mechanical isolation and interest for plastic surgery. *Ann Chir Plast Esthet*. 2019;64:1-10.
53. Senesi L, De Francesco F, Fariñelli L, et al. Mechanical and enzymatic procedures to isolate the stromal vascular fraction from adipose tissue: preliminary results. *Front Cell Dev Biol*. 2019;7:88.
54. De Francesco F, Tirino V, Desiderio V, et al. Human CD34/CD90 ASCs are capable of growing as sphere clusters, producing high levels of VEGF and forming capillaries. *PLoS One*. 2009;4(8):e6537.
55. Zannettino AC, Paton S, Arthur A, et al. Multipotential human adipose-derived stromal stem cells exhibit a perivascular phenotype in vitro and in vivo. *J Cell Physiol*. 2008;214(2):413-421.
56. Mizuno H. The potential for treatment of skeletal muscle disorders with adipose-derived stem cells. *Curr Stem Cell Res Ther*. 2010;5(2):133-136.
57. Polly SS, Nichols AEC, Donnini E, et al. Adipose-derived stromal vascular fraction and cultured stromal cells as trophic mediators for tendon healing. *J Orthop Res*. 2019;37(6):1429-1439.
58. Behfar M, Sarrafzadeh-Rezaei F, Hobbenghi R, et al. Adipose-derived stromal vascular fraction improves tendon healing in rabbits. *Chin J Traumatol*. 2011;14(6):329-335.
59. Ghiasloo M, Lobato RC, Diaz JM, et al. Expanding clinical indications of mechanically isolated stromal vascular fraction: a systematic review. *Aesthet Surg J*. 2020;40(9):NP546-NP560.

60. Behfar M, Sarrafzadeh-Rezaei F, Hobbenaghi R, et al. Enhanced mechanical properties of rabbit flexor tendons in response to intratendinous injection of adipose derived stromal vascular fraction. *Curr Stem Cell Res Ther*. 2012;7(3):173-178.
61. Lu LY, Ma M, Cai JF, et al. Effects of local application of adipose-derived stromal vascular fraction on tendon-bone healing after rotator cuff tear in rabbits. *Chin Med J (Engl)*. 2018;131(21):2620-2622.
62. Albano D, Messina C, Usuelli FG, et al. Magnetic resonance and ultrasound in Achilles tendinopathy: predictive role and response assessment to platelet-rich plasma and adipose-derived stromal vascular fraction injection. *Eur J Radiol*. 2017;95:130-135.
63. Usuelli FG, Grassi M, Maccario C, et al. Intratendinous adipose-derived stromal vascular fraction (SVF) injection provides a safe, efficacious treatment for Achilles tendinopathy: results of a randomized controlled clinical trial at a 6-month follow-up. *Knee Surg Sports Traumatol Arthrosc*. 2018;26(7):2000-2010.
64. Archambault JM, Wiley JP, Bray RC, et al. Can sonography predict the outcome in patients with achillobodynia? *J Clin Ultrasound*. 1998;26(7):335-339.
65. Dirrachs T, Quack V, Gatz M, et al. Shear wave elastography (SWE) for the evaluation of patients with tendinopathies. *Acad Radiol*. 2016;23:1204-1213.
66. Aubry S, Nueffer JP, Tanter M, et al. Viscoelasticity in Achilles tendonopathy: quantitative assessment by using real-time shear-wave elastography. *Radiology*. 2015;274:821-829.
67. Coombes BK, Tucker K, Vicenzino B, et al. Achilles and patellar tendinopathy display opposite changes in elastic properties: a shear wave elastography study. *Scand J Med Sci Sports*. 2018;28:1201-1208.
68. Ahn KS, Lee NJ, Kang CH, et al. Serial changes of tendon histomorphology and strain elastography after induced Achilles tendinopathy in rabbits: an in vivo study. *J Ultrasound Med*. 2017;36(4):767-774.
69. Loebel C, Burdick JA. Engineering stem and stromal cell therapies for musculoskeletal tissue repair. *Cell Stem Cell*. 2018;22:325-339.
70. Wang Y, Chen X, Cao W, et al. Plasticity of mesenchymal stem cells in immunomodulation: pathological and therapeutic implications. *Nat Immunol*. 2014;15:1009-1016.
71. Caplan AI, Dennis JE. Mesenchymal stem cells as trophic mediators. *J Cell Biochem*. 2006;98:1076-1084.
72. D'Andrea F, De Francesco F, Ferraro GA, et al. Large-scale production of human adipose tissue from stem cells: a new tool for regenerative medicine and tissue banking. *Tissue Eng Part C Methods*. 2008;14:233-242.
73. Ferraro GA, De Francesco F, Nicoletti G, et al. Human adipose CD34 + CD90+ stem cells and collagen scaffold constructs grafted in vivo fabricate loose connective and adipose tissues. *J Cell Biochem*. 2013;114:1039-1049.
74. Nicoletti GF, De Francesco F, D'Andrea F, et al. Methods and procedures in adipose stem cells: state of the art and perspective for translation medicine. *J Cell Physiol*. 2015;230:489-495.
75. Lacitignola L, Staffieri F, Rossi G, et al. Survival of bone marrow mesenchymal stem cells labelled with red fluorescent protein in an ovine model of collagenase-induced tendinitis. *Vet Comp OrthopTraumatol*. 2014;27:204-209.
76. Dirks R, Warden S. Models for the study of tendinopathy. *J Musculoskelet Neuronal Interact*. 2011;11:141-149.
77. Geburek F, Roggel F, van Schie HTM, et al. Effect of single intralesional treatment of surgically induced equine superficial digital flexor tendon core lesions with adipose-derived mesenchymal stromal cells: a controlled experimental trial. *Stem Cell Res Ther*. 2017;8(1):129.
78. Chen HS, Su YT, Chan TM, et al. Human adipose-derived stem cells accelerate the restoration of tensile strength of tendon and alleviate the progression of rotator cuff injury in a rat model. *Cell Transplant*. 2015;24(3):509-520.
79. Watts AE, Nixon AJ, Yeager AE, et al. A collagenase gel/physical defect model for controlled induction of superficial digital flexor tendonitis. *Equine Vet J*. 2012;44:576-586.
80. Falomo ME, Ferroni L, Tocco I, et al. Immunomodulatory role of adipose-derived stem cells on equine endometriosis. *Biomed Res Int*. 2015;2015:141485.
81. Uysal CA, Tobita M, Hyakusoku H, et al. Adipose-derived stem cells enhance primary tendon repair: biomechanical and immunohistochemical evaluation. *J Plast Reconstr Aesthet Surg*. 2012;65(12):1712-1719.
82. Valencia Mora M, Antuña Antuña S, García Arranz M, Carrascal MT, Barco R. Application of adipose tissue-derived stem cells in a rat rotator cuff repair model. *Injury*. 2014;45(suppl 4):S22-S27.
83. Viganò M, Lugano G, Perucca Orfei C, et al. Autologous micro-fragmented adipose tissue reduces the catabolic and fibrosis response in an in vitro model of tendon cell inflammation. *Stem Cells Int*. 2019;2019:5620286.
84. Costa-Almeida R, Calejo I, Reis RL, Gomes ME. Crosstalk between adipose stem cells and tendon cells reveals a temporal regulation of tenogenesis by matrix deposition and remodeling. *J Cell Physiol*. 2018;233(7):5383-5395.
85. Francisco V, Pino J, Gonzalez-Gay MA, et al. Adipokines and inflammation: is it a question of weight? *Br J Pharmacol*. 2018;175:1569-1579.
86. de Girolamo L, Grassi M, Viganò M, et al. Treatment of Achilles tendinopathy with autologous adipose-derived stromal vascular fraction: results of a randomized prospective clinical trial. *Orthop J Sports Medicine*. 2016;4(7):supplement 4.
87. Chiou GJ, Crowe C, McGoldrick R, et al. Optimization of an injectable tendon hydrogel: the effects of platelet-rich plasma and adipose-derived stem cells on tendon healing in vivo. *Tissue Eng Part A*. 2015;21(9-10):1579-1586.

SUPPORTING INFORMATION

Additional supporting information may be found online in the Supporting Information section at the end of this article.

How to cite this article: Palumbo Piccionello A, Riccio V, Senesi L, et al. Adipose micro-grafts enhance tendinopathy healing in ovine model: An in vivo experimental perspective study. *STEM CELLS Transl Med*. 2021;10(11):1544-1560.

<https://doi.org/10.1002/sctm.20-0496>